COMPOSITION EFFECTS ON THE MECHANICAL PROPERTIES OF MICROEMULSION-MADE CORE/SHELL POLYMERS.

M. Rabelero[1, *], M. Puca[1], E. Mendizábal[1], R.G. López[2] and J.E. Puig[1]

1Departamentos de Química e Ingeniería Química, Universidad de Guadalajara, Boul. M. García Barragán # 1451, Guadalajara, Jal. 44430 – mrabelero@hotmail.
[2]Centro de Investigaciones en Química Aplicada, Saltillo, Coah. 25100.

Abstract- The synthesis of hard-core/soft-shell and soft-core/hard-shell polymers by a two-stage semi-continuous microemulsion polymerization process is reported here. In the first stage, high-solid polymer seeds (> 30 wt. %) of slightly crosslinked polystyrene or poly(butyl acrylate) were obtained; then, the other monomer was added semi-continuously to form the shell. The effects on the mechanical properties (Young's modulus, ultimate properties, hardness and impact energy) of the ratio of rigid-to-soft and soft-to-rigid polymers were studied. It was found that the material becomes stiffer and presents a lower elongation at break as the amount of the rigid polymer increases. The mechanical properties also depend on the location of the hard and soft polymers. Experimental mechanical properties were compared with the predictions of the Kerner and the equivalent box models. Predictions of the Kerner model suggests that phase inversion occurred in the case of hard-core/soft-shell materials, it was corroborated by transmission electron microscopy. The thermodynamically preferred morphology, is that of soft-core/hard-shell, regardless of the order of addition of monomers. Experimental data follow closely the predictions of the Equivalent Box model only for soft-core/hard-shell polymers.

Introduction

Core/shell polymers typically consist of at least two main polymeric domains: one usually having a low-glass transition temperature (T_g) and another with a high-T_g, respectively, than the working temperature [1-2]. Core/shell polymer particles can be used in a wide range of applications because they exhibit tunable and/or improved chemical and mechanical properties compared to those of the parent-component polymers [3]. Core/shell particles differing in glass transition temperatures are used in coatings and non-porous homogeneous films [4, 5], as modifiers of the mechanical properties of thermoplastics [6-8] and in the manufacture of nanocomposite materials [9]. Typically, a two-stage emulsion polymerization process is used to produce core/shell polymers [1, 4, 5, 7].

Microemulsion polymerization is an alternative process for producing core/shell polymer particles of nano-size scale [10]. In this process, latexes containing tiny particles (< 50 nm), each composed of a few macromolecules of high molecular weight (>10^6 Dalton), are produced [11-13], over which other(s) monomer(s) can be added in batch or semi-continuously to form the shell [10].

In this work we report the synthesis by microemulsion polymerization and the mechanical properties of hard-core/soft-shell and soft-core/hard-shell polymers as a function of the ratio of the two forming polymers–poly(butyl acrylate) and polystyrene. The seed latexes were made by adding more monomer in a semi-continuous fashion to increase the solid content. Then the second monomer was also added semi-continuously to form the shell. The mechanical properties (stress-strain, hardness and impact tests) are reported and compared with predictions of the Equivalent Box and the Kerner models.

Experimental

A two-stage semi-continuous microemulsion polymerization process was used for the synthesis of the core/shell polymers. First, microemulsions containing 14.1 wt. % DTAB, 79.9 wt. % H_2O and 6 wt. % styrene or butyl acrylate were polymerized at 60°C with V-50 ($w_{V\text{-}50}/w_{monomer}$ = 0.01) in the presence of small amounts of ALMA ($w_{ALMA}/w_{monomer}$ = 0.01) to produce slightly crosslinked

particles. To increase the solid content in the latexes, more monomer was added semi-continuously for over 6 hours. The latex is diluted with water to 10% solids and used as the seed in the second stage. The required amount of BA (or St) to obtain the desired composition was added in the second stage to form the shell. Polymer was precipitated by adding methanol, washed, and dried. Glass transition temperatures (T_g) were obtained with a DSC-7 Perkin-Elmer differential scanning calorimeter. Particle size was measured with a Malvern 4700C QLS. The microstructures of the composite latex particles were examined in a JEOL 1010 electron transmission microscope. To improve the contrast, samples were treated with a 1 % phosphotungstic acid solution. Polymer bars (10 x 63 x 2 mm) for the tensile tests were made by heating at 120°C and pressing at 150 bars. Tensile tests were performed according to the ASTM D-638 method at an elongation velocity of 2 in/min in an universal testing machine from United. Shore hardness "A" was measured according to the ASTM D2240 method with a 306 L PTC Instrument and impact tests according to the ASTM D-1709 method in a CS-126G Custom Scientific Instrument.

Results and Discussion

Table 1 reports the conversions, % solids, the QLSz-average particle size in stages 1 and 2, an estimation of a theoretical particle size and the volume fracction of the differents polymers prepared here. Final conversions are high (> 90 %). At the end of the first stage, all the latexes had a solid content higher than 30% and contain particles of about 42 to 47 nm in diameter, characteristic of microemulsion polymerization [11, 14]. At the end of the second stage, particle size has increased but it remains within the range of microemulsion-made. This growth suggests that the monomer added during the second stage polymerizes over the seed particles. To estimate the amount of the second monomer incorporated over the seeds, we compared the z-average particle size with a *theoretical* value, estimated by knowing the amount of the monomer added in the second stage, the conversion, and the density of the polymer in the shell. Calculated and measured average particle diameters are fairly close in most cases. The *actual* volume fraction – based on the polymer produced in the second stage, was calculated from the measured particle diameters at the end of the first and second stages. In what follows, we will use the *actual* polymer volume fraction (ϕ_2).

DSC detected two glass transition temperatures, which is an indication of the presence of two segregated polymer phases in the material. The lower one (≈ –50°C) corresponds to poly(butyl acrylate) whereas the higher one (≈ 100°C) corresponds to polystyrene.

Figure 1 shows the stress-strain curves of PBA-core/PSt-shell polymers made by microemulsion polymerization. The sample with highest PSt content (PBA/PSt = 40/60) is rigid and breaks before yielding, with a smaller tensile stress at break (ca. 10 MPa) than polystyrene (36 MPa), but a slightly larger elongation at break (inset in Fig. 1). As the concentration of PSt decreases, the polymer become softer and more elastic. The yielding point decreases to ca. 6 MPa for the 60/40-sample and to ca. 1 MPa for the 70/30-sample, whereas the elongation at break increases from 53 to 75 % for these samples, respectively. Hence, the behavior changes from rigid to elastic upon increasing the amount of PBA in the core.

Figure 2 depicts the stress-strain curves of the PSt-core/PBA-shell polymers. The sample with PBA/PSt = 40/60 has an elastic behavior with a yield stress at ca. 0.8 MPa and an elongation at break of 150%. Samples with 50/50 and 60/40 exhibit a yield point (inset of Fig. 2) followed by a small region of elongation at constant stress and then stress softening with ultimate stress values much lower than their corresponding yield stresses. The sample with highest PSt content (30/70) is rigid and breaks at a stress of 15 MPa.

Figure 3 reports the tensile modulus versus PSt composition for core/shell polymers. The polymers with the hard-shell exhibit higher modulus at all compositions. The predictions of the equivalent box model (EBM) [15], are reported in Figure 3 as a solid line. The volume fraction contributions of the EBM can be calculated by the percolation theory for the tensile modulus of a two-component

blend with a negligible contribution of the second component. The predictions of the EBM were done using the universal constants [15] and the experimental modulus of the homo-polymers measured in our laboratory. Predictions agree well with experimental tensile modulus of the soft-core/hard-shell. On the other hand, experimental modulus of the hard-core/soft-shell polymers deviates considerably from the predictions of the model. In this case, the experimental data fall below the predictions and deviations become larger as the PSt content diminishes.

Figure 4 depicts the comparison between experimental and the Kerner predictions [16] assuming that either PSt or PBA is the continuous phase. The predictions assuming that PSt is the continuous phase agree well with the PBA/PSt materials with $\phi_{PSt} \geq 0.4$. For lower volume fractions, Kerner over-predicts the modulus. On the other hand, with the assumption that PBA is the continuous phase in the PSt/PBA, the model predictions deviate from the experimental values. Notice, however, that the data tend to approach the Kerner model predictions with the assumption that PSt is the continuous phase. These results suggest that a phase inversion or a disruption of the core/shell structure may occur.

To investigate further this issue, we applied the theory of Sundberg *et al.* [17], in which the thermodynamically preferred morphology is the one with a minimum interfacial free energy change among four possible equilibrium morphologies, namely, core/shell (*CS*), inverted core/shell (*ICS*), individual particles(*IP*) and hemisphere [18]. Table 2 summarizes the calculations of the interfacial free energy change of the core/shell examined. When PBA forms the seeds, the minimum interfacial free energy change corresponds to the core/shell structure, i.e. the PSt incorporates over the seeds. This PBA-core/PSt-shell morphology is confirmed by TEM, where the dark domains correspond to PSt and the light domains to PBA (Figure 5). However, when PSt forms the seeds, the minimum interfacial free energy change corresponds to the inverted core/shell structure, so phase inversion should occur. Figure 6 shows that in this case also the PSt (dark domains) is in the outer layer, although incomplete inverted core/shell morphology is observed. Hence, we have to conclude, based on this analysis and TEM observations, that PSt is mainly located in the shell of these materials notwithstanding the order of addition of the monomers during the preparation of the core/shell structure. However, the mechanical properties of polymers with similar weight ratio of PSt and PBA depend on the order of addition, which suggests that the inversion may not be complete. Hence, it is likely that incomplete inversion occurred for the PSt/PBA particles, which can explain the lower mechanical properties compared to the "thermodynamically favored" PBA/PSt particles. Indeed, Figure 6 confirms that incomplete inversion occurs. Table 3 shows the main mechanical properties of the polymer prepared here.

Table 1. Conversions, solid content, average particle size at the end of stages 1 and 2, and volume fraction of polymer formed during the second stage, for the core-shell polymers prepared by microemulsion polymerization. [(a)]Measured by QLS; [(b)]estimated with considerations; [(c)]estimated with actual diameter; [(d)]estimated with expected diameter.

Core/shell Composition	Conversion (%) Stage 1	Conversion (%) Stage 2	% Solids Stage 1	Dp_z (nm) Stage 1	% Solids Stage 2	Dp_z (nm) [(a)] Stage 2	Dp_z (nm) [(b)] Stage 2	ϕ [(c)]	ϕ [(d)]
PSt/PBA 70/30	94.3	98.9	32.4	42.0	15.0	45.3	47.7	0.203	0.317
PSt/PBA 60/40	94.3	94.8	32.4	42.0	16.3	45.8	49.5	0.229	0.389
PSt/PBA 50/50	93.8	99.7	39.2	47.3	19.8	58.2	60.6	0.463	0.525
PSt/PBA 40/60	93.8	94.3	39.2	47.3	22.7	59.2	63.9	0.49	0.594
PBA/PSt 70/30	96.0	94.1	39.0	41.7	14.5	46.9	47.0	0.297	0.30
PBA/PSt 60/40	96.0	96.3	39.0	41.7	16.9	49.9	50.1	0.416	0.423
PBA/PSt 50/50	96.0	90.6	39.0	41.7	18.3	51.2	51.8	0.458	0.478
PBA/PSt 40/60	96.0	90.7	39.0	41.7	19.3	53.8	56.6	0.534	0.6

Table 2. Interfacial free energy changes for different morphologies of the different core/shell compositions prepared here.

Core/shell Composition	$(\Delta\gamma)_{CS}$ (mN/m)	$(\Delta\gamma)_{ICS}$ (mN/m)	$(\Delta\gamma)_{IP}$ (mN/m)	Predicted morphology
PSt/PBA 70/30	7.96	3.85	9.21	ICS
PSt/PBA 60/40	8.56	4.44	10.21	ICS
PSt/PBA 50/50	16.00	11.62	20.77	ICS
PSt/PBA 40/60	17.22	12.78	22.33	ICS
PBA/PSt 70/30	3.93	6.86	11.33	CS
PBA/PSt 60/40	7.29	11.02	19.84	CS
PBA/PSt 50/50	8.95	12.83	18.0	CS
PBA/PSt 40/60	11.99	16.79	21.5	CS

Table 3. Mechanical properties as a function of composition

Composition core/shell	Young Modulus (MPa)	Ultimate Strain (%)	Tensile Stress (MPa)	Hardness Shore A	Impact energy (J/cm)
PSt/PBA 70/30	877.2	1.9	14.6	95.8	0.1
PSt/PBA 60/40	312.5	29.5	6.5	92.2	0.3
PSt/PBA 50/50	166.7	22.9	4.4	81.0	1.8
PSt/PBA 40/60	53.6	137.3	3.1	59.2	24.0
PSt/PBA 30/70	0.8	276.8	0.4	21.8	16.2
PBA/PSt 70/30	10.0	73.3	1.4	60.8	11.9
PBA/PSt 60/40	178.6	54.5	7.2	83.7	14.3
PBA/PSt 50/50	401.6	33.0	13.5	85.7	1.2
PBA/PSt 40/60	606.1	1.7	9.5	91.0	0.07

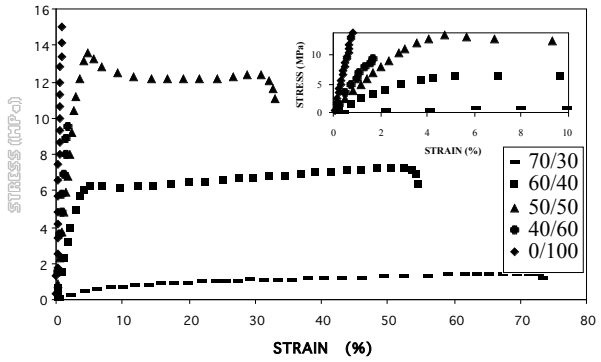

Figure 1 Stress-strain data for PBA-core/PSt-shell polymers of different PBA/PSt ratios.

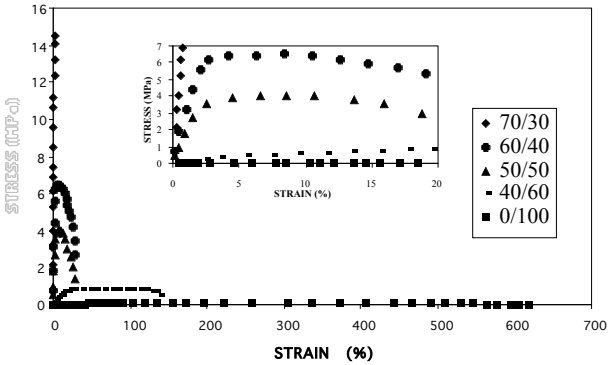

Figure 2. Stress-strain data for PSt-core/PBA-shell polymers with different PSt/PBA ratios.

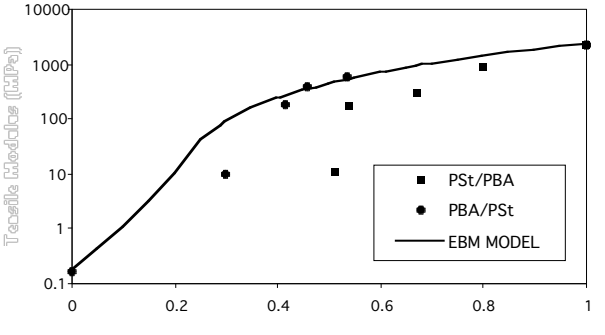

Figure 3. Tensile modulus versus PSt volume fractions for PBA-core/PSt-shell (●) and PSt-core/PBA-shell (■) polymers. Solid line represents the predictions of the equivalent box model.

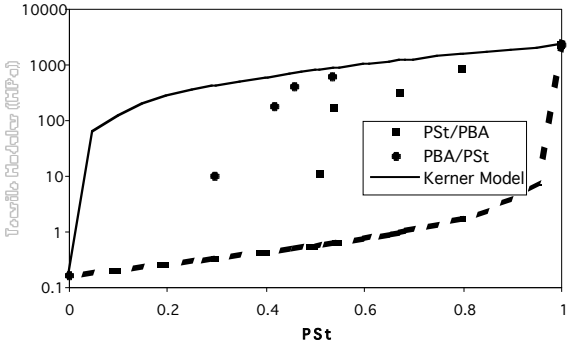

Figure 4. Tensile modulus versus PSt volume fractions for PBA-core/PSt-shell (●) and PSt-core/PBA-shell (■) polymers. Predictions of the Kerner model assuming that PBA (solid) or PSt (dashed) is the continuous phase.

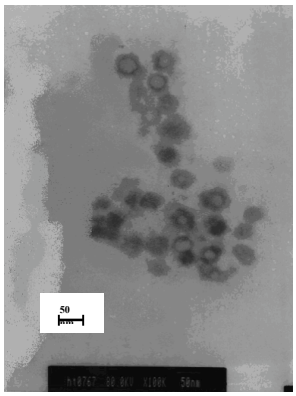

Figure 5. TEM photography of PBA/PSt core/shell polymer particles

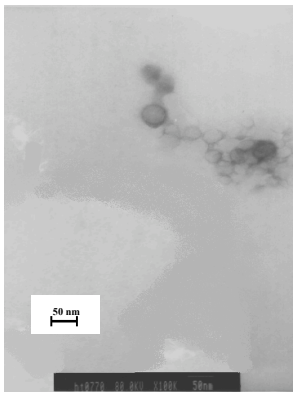

Figure 6. TEM photography of PSt/PBA core/shell polymer particles

Concluding Remarks

In this work we demonstrated that is possible to obtain core-shell polymers of polystyrene/poly(butyl acrylate) with high solid content by a two-stage microemulsion polymerization. Elsewhere we reported that PSt-core/PBA-shell polymers made by microemulsion polymerization were tougher and with similar elongations at break than emulsion-made polymers of similar composition [10]. Our results indicate that by varying the core-shell composition and the initial location of the polymers, it is possible to obtain materials with a broad range of mechanical properties. These polymer particles are promising for using in coatings, adhesives or impact-resistance plastics due to their mechanical characteristics and small sizes.

Acknowledgements

This work was supported by the Consejo Nacional de Ciencia y Tecnología (Grant # 38725-U).

References

1. Rios L, Hidalgo M., Cavaille J. Y., Guillot J., Guyot A. and Pichot C., *Colloid Polym. Sci*. 1991, **269**: 812-824.
2. Lee S., Rudin A., In: Daniels E., Sudol Ed., El-Aasser M. S., editors, *Polymer Latexes*, *ACS Symposium Series* 1992; 492: 234.
3. Lu M., Keskkula H. and Paul D. R., *Polymer* 1996; 37: 125-135.
4. Hidalgo M., Cavaille J. Y., Guillot J., Guyot A., Pichot C., Rios L., Vassoille R., *Coll. Polym. Sci.* 1992; 270:1208-1221.
5. Mendizábal E., Hernández-Patiño P. J., Puig J. E., Canché-Escamilla G., Katime I., Castaño V., *J. Appl. Polym. Sci.* 1999; 74 (14): 3299-3304.
6. Qian J. Y., Pearson R. A., Dimonie V. L., El-Aasser M. S., *J. Appl Polym Sci* 1995; 58 (2): 439-448.
7. Ha J. W., Park I. J., Lee S. B., Kim D. K., *Macromolecules* 2002; 35 (18): 6811-6818.
8. Ferguson C. J., Russell G. T., Gilbert R. G., *Polymer* 2002; 43 (24): 6371-6382.
9. Kalinina E., Kumacheva E., *Macromolecules* 2001; 34 (18): 6380-6386.
10. Aguiar A., Gonzalez-Villegas S., Rabelero M., Mendizábal E., Puig J. E., *Macromolecules* 1999; 32 (20): 6767-6771.
11. Puig J. E. In: Salamone J. P., editor. *Polymeric Materials Encyclopedia*, vol. 6, Boca Raton: CRC Press, 1996; 4333-4341.
12. Candau F. In: *Handbook of Microemulsion Science and Technology,* Kumar P, Mittal KL, editors. New York: Marcel Dekker. 1999; 679-712.
13. Candau F. In: Paleos CM, editor, *Polymerization in Organized Media*, Philadelphia: Gordon Breach Sci. Pub., 1992.
14. Puig J. E., *Rev. Mex. Fis*. 1999, 45 Suppl: 18.
15. Robeson L. M., Berner R. A., *J. Polym. Sci. B, Polym Phys* 2001; 39: 1093-1106.
16. Kerner E. H., *Proc. Phys. Soc. London. Sect. B*, 1956; 69B: 808-813.
17. Sundberg D. C., Casassa A. P., Pantazopoulos J., Muscato M. R., *J. Appl. Polym. Sci*. 1990; 41: 1425-1442.
18. Zhao K., Sun P., Liu D., Wang L., *J. Appl. Polym. Sci*. 2004; 92: 3144-3152.